

Bjorken flow in one-dimensional relativistic magnetohydrodynamics with magnetization

Shi Pu¹, Victor Roy¹, Luciano Rezzolla^{1,2}, and Dirk H. Rischke¹

¹ *Institute for Theoretical Physics, Goethe University,
Max-von-Laue-Str. 1, 60438 Frankfurt am Main, Germany and*

² *Frankfurt Institute for Advanced Studies, Goethe University,
Ruth-Moufang-Str. 1, 60438 Frankfurt am Main, Germany*

We study the one-dimensional, longitudinally boost-invariant motion of an ideal fluid with infinite conductivity in the presence of a transverse magnetic field, i.e., in the ideal transverse magnetohydrodynamical limit. In an extension of our previous work Roy et al., [Phys. Lett. B 750, 45 (2015)], we consider the fluid to have a non-zero magnetization. First, we assume a constant magnetic susceptibility χ_m and consider an ultrarelativistic ideal gas equation of state. For a paramagnetic fluid (i.e., with $\chi_m > 0$), the decay of the energy density slows down since the fluid gains energy from the magnetic field. For a diamagnetic fluid (i.e., with $\chi_m < 0$), the energy density decays faster because it feeds energy into the magnetic field. Furthermore, when the magnetic field is taken to be external and to decay in proper time τ with a power law $\sim \tau^{-a}$, two distinct solutions can be found depending on the values of a and χ_m . Finally, we also solve the ideal magnetohydrodynamical equations for one-dimensional Bjorken flow with a temperature-dependent magnetic susceptibility and a realistic equation of state given by lattice-QCD data. We find that the temperature and energy density decay more slowly because of the non-vanishing magnetization. For values of the magnetic field typical for heavy-ion collisions, this effect is, however, rather small. Only for magnetic fields which are about an order of magnitude larger than expected for heavy-ion collisions, the system is substantially reheated and the lifetime of the quark phase might be extended.

I. INTRODUCTION

It has recently been pointed out that extremely strong magnetic fields are produced in relativistic heavy-ion collisions. In general, their magnitude grows approximately linearly with the centre-of-momentum energy of the colliding nucleons [1–3], and reaches $B \sim 10^{18} - 10^{19}$ G in Au-Au collisions at $\sqrt{s_{NN}} = 200$ GeV. In these collisions a new form of hot and dense nuclear matter is created, commonly known as quark-gluon plasma (QGP) [4]. In the QGP, quarks are deconfined and chiral symmetry is restored, such that quarks are (approximately) massless and have definite chirality and helicity. Thus, in the presence of very strong magnetic fields, quarks will be polarized and will move preferentially in the direction parallel (or antiparallel) to the magnetic field. Therefore, if the numbers of left- and right-handed quarks are not equal, a net charge current will be induced, a phenomenon known as “chiral magnetic effect” (CME) [5, 6]. As well as charge currents, a chiral current can also be induced by the magnetic field and gives rise to the “chiral separation effect” (CSE). Combining these two effects, a density wave is expected to be induced by magnetic fields, called “chiral magnetic wave” (CMW) [7], which might break the degeneracy between the elliptic flows of π^\pm [8]. Recently, it has been found that these phenomena can be interpreted in the language of the Berry phase and effective chiral kinetic equations, which can be obtained by the path-integral method [9–11], Hamiltonian approaches [12, 13], and quantum kinetic theory via Wigner functions [14, 15]; for reviews and additional references see Refs. [16–19].

A possible origin of CME, CSE, and CMW is the chiral anomaly, which is topologically invariant. Thus, these effects are not expected to be significantly modified when considering interactions between particles. In contrast, there are also several interesting phenomena dominated by the interactions.

For example, instead of a strong magnetic field, a chiral current and density wave can also be induced by an electric field, the so-called “chiral electric separation effect” (CESE) [20–23]. Similarly, adding an electric field perpendicular to the magnetic field, a chiral Hall current is expected, called “chiral Hall-separation effect” (CHSE) [23], which might cause an asymmetric charge and chirality distribution in rapidity. These phenomena have drawn considerable attention within the study of hot and dense matter under the influence of strong magnetic fields.

A very popular and successful tool to describe heavy-ion collision dynamics is relativistic hydrodynamics [see, e.g., Refs. [24–31]]. In order to study some of the phenomena mentioned above within a hydrodynamical approach, the latter needs to be extended to include magnetic fields, i.e., one has to develop and apply a relativistic magnetohydrodynamical (MHD) framework. Although the magnetic field created in heavy-ion collisions rapidly decays in the vacuum [5] and might become very small even before the system reaches local thermal equilibrium, some recent studies have shown that its decay might be substantially delayed in the presence of an electrically conducting medium [32–34]. Thus, it is still presently unclear whether the effect of magnetic fields on the dynamics of a heavy-ion collision can be neglected or needs to be taken properly into account.

In analogy with our previous work [35] (hereafter paper I), we define the dimensionless quantity, $\sigma = B^2/e$, to measure the relative importance of the magnetic field, with B being the magnitude of the magnetic field (measured in units of GeV^2) and e the energy density of the fluid. Clearly, for regions where $\sigma \gtrsim 1$, the effect of the magnetic fields cannot be ignored. Interestingly, in a typical mid-central Au-Au collision (e.g., with impact parameter ~ 10 fm at $\sqrt{s_{NN}} = 200$ GeV), the average magnetic field is $\sim 10 m_\pi^2$ [1, 2], with m_π the pion mass, and the energy density is $\sim 10 \text{ GeV fm}^{-3}$, thus giving

$\sigma \sim 0.5$. Furthermore, event-by-event simulations show that in certain events σ could be even much larger than 1 in certain regions [36]. Therefore, it is still very important to investigate relativistic MHD, ideally with a numerical code solving the equations in 3+1 dimensions.

Before starting to investigate MHD numerically, it is worth while to search for analytic solutions in some simple, but nevertheless realistic test cases. In paper I we have considered one-dimensional, longitudinally boost-invariant Bjorken flow [37] with a transverse magnetic field and in ideal MHD, i.e., for infinite electrical conductivity and without dissipative effects. Quite remarkably, we found that under these conditions the decay of the energy density is the same as in the case without magnetic field. The reason is that, for a transverse magnetic field, B/s (where s is the entropy density) is conserved and the magnetic field is advected with the fluid, as a manifestation of the "frozen-flux theorem" well-known from astrophysics and plasma physics [31, 38].

In paper I we have neglected the effect of a nonzero magnetization of the QGP. In this work, we extend our previous study to include a nonzero magnetization for the scenario of a pure Bjorken flow. The final goals are those of improving the theoretical understanding of the MHD evolution of the QGP, but also of determining how the magnetization of the QGP may have an influence on measurable quantities, as recently suggested in Ref. [39] in relation to the value of the elliptic flow parameter v_2 .

Within a linear approximation, the magnetization effect can be described through the magnetic susceptibility χ_m , which is the ratio of the magnetic polarization to the magnetic field¹. Interestingly, numerous studies, e.g., from lattice QCD [39, 44–49] and from perturbative QCD [50], using the Sakai-Sugimoto model [51], the functional renormalization group [50], or other models [48, 52–56], have all suggested that in a confined phase (hadron phase) the medium is diamagnetic, i.e., with $\chi_m < 0$, while in the deconfined QGP phase it is paramagnetic, i.e., with $\chi_m > 0$. As a result, by simply choosing different signs of χ_m , we can investigate the dynamics of different phases with nonzero magnetization.

In principle, the magnetic susceptibility χ_m of the QGP is a function of the temperature and of the magnitude of the magnetic field. In practice, however, the variation of χ_m is very small in the experimentally accessible region of temperatures and magnetic fields. For example, from lattice-QCD calculations [39, 45] [see also Ref. [48]], for $(eB)^2 = 0.007 - 0.2 \text{ GeV}^2$ and $T = 100 - 350 \text{ MeV}$, the susceptibility is in the range $0 \lesssim \chi_m \lesssim 0.05$ [note that a prefactor $4\pi\alpha$ is required to convert the values of Refs. [39, 45, 48] from SI to natural units]. In view of this and for the sake of simplicity, we will first assume a constant χ_m and then investigate the modifica-

tions of the dynamics when χ_m is assumed to depend on the temperature.

This paper is organized as follows. In Sec. II, we introduce the ideal-MHD framework with nonzero magnetization. We also discuss the conservation equations and apply them to Bjorken flow in the presence of a magnetic field. In Sec. III, we obtain the temporal evolution of the energy density in ideal transverse MHD with magnetization. As a useful comparison, we consider in Sec. IV the decay of the energy density in the presence of an external magnetic field undergoing a power-law decay in proper time. In Sec. V we solve the MHD equations numerically for a temperature-dependent magnetic susceptibility and a realistic equation of state (EOS). Finally, we summarize and conclude in Sec. VI.

Throughout this work, we work in a flat spacetime with the metric tensor $g_{\mu\nu} = \eta_{\mu\nu} = \text{diag}\{+, -, -, -\}$, so that the fluid four-velocity u^μ satisfies $u^\mu u_\mu = 1$ and the orthogonal projector to the fluid four-velocity is defined as $\Delta^{\mu\nu} = g^{\mu\nu} - u^\mu u^\nu$. We will also use the Levi-Civita tensor with $\epsilon^{0123} = -\epsilon_{0123} = 1$. Note that in this convention, contracting the indices of two Levi-Civita tensors will have an additional minus sign, e.g., $\epsilon^{\mu\nu\alpha\beta} \epsilon_{\mu\nu\rho\sigma} = -(g_\rho^\alpha g_\sigma^\beta - g_\sigma^\alpha g_\rho^\beta)$.

II. IDEAL MHD WITH MAGNETIZATION

A. Covariant form of the MHD equations

In this section, we give a brief introduction to the Lorentz-covariant form of ideal MHD with nonzero magnetization. More details can be found in Refs. [57–60], which use the same convention as this work, or in Refs. [61, 62], which use instead a +2 signature for the metric.

We start by recalling that in the presence of an electromagnetic field, the (total) energy-momentum tensor of an ideal fluid can be decomposed into two parts

$$T^{\mu\nu} = T_M^{\mu\nu} + T_{EM}^{\mu\nu}, \quad (1)$$

where

$$T_{EM}^{\mu\nu} = -F^{\mu\lambda} F_\lambda^\nu + \frac{1}{4} g^{\mu\nu} F^{\alpha\beta} F_{\alpha\beta}, \quad (2)$$

is the contribution from the electromagnetic fields and

$$T_M^{\mu\nu} = e u^\mu u^\nu - p \Delta^{\mu\nu} - \frac{1}{2} (M^{\mu\lambda} F_\lambda^\nu + M^{\nu\lambda} F_\lambda^\mu), \quad (3)$$

refers to the matter part, with p being the thermodynamic pressure [31]. The polarization tensor $M^{\mu\nu}$ can be expressed directly through the derivatives of the grand canonical potential Ω with respect to the electromagnetic field (or Faraday tensor) $F^{\mu\nu}$ as

$$M^{\mu\nu} \equiv -\frac{\partial\Omega(T, \mu, B)}{\partial F_{\mu\nu}}, \quad (4)$$

where T, μ, B are the temperature, the chemical potential, and the strength of the magnetic field, respectively. In the weak-field limit, the terms $\sim M^{\mu\nu}$ in Eq. (3) can be neglected.

¹ Note that usually the magnetic susceptibility is related to the quark condensate $\langle \bar{\psi} \sigma_{\mu\nu} \psi \rangle$ [40], and has been studied in a number of works, see e.g., Refs. [41, 42] for lattice QCD, Ref. [43] for other theoretical studies. Here, we concentrate on the *full* magnetic susceptibility, which is defined through a derivative of the pressure (grand canonical potential); more details will be discussed in Sec. II.

The equations for the conservation of the (total) energy and momentum are given simply by

$$\partial_\mu T^{\mu\nu} = 0, \quad (5)$$

and reduce, with the help of Maxwell's equations, to the well-known form

$$\partial_\mu T_M^{\mu\nu} = -\partial_\mu T_{EM}^{\mu\nu} = F^{\mu\lambda} j_\lambda, \quad (6)$$

with j^μ being the charge current. Without loss of generality, the electromagnetic field tensor can be decomposed as

$$F^{\mu\nu} = E^\mu u^\nu - E^\nu u^\mu + \epsilon^{\mu\nu\alpha\beta} u_\alpha B_\beta, \quad (7)$$

with

$$E^\mu \equiv F^{\mu\nu} u_\nu, \quad B^\mu \equiv \frac{1}{2} \epsilon^{\mu\nu\alpha\beta} u_\nu F_{\alpha\beta}. \quad (8)$$

In the local rest frame of the fluid, where $u^\mu = (1, \mathbf{0})$, the spatial components of E^μ represent the electric-field three-vector, while those of B^μ refer to magnetic-field three-vector. We can next introduce the in-medium field-strength tensor $H^{\mu\nu} \equiv F^{\mu\nu} - M^{\mu\nu}$ and similarly decompose $H^{\mu\nu}$ and $M^{\mu\nu}$ as

$$\begin{aligned} M^{\mu\nu} &= P^\nu u^\mu - P^\mu u^\nu + \epsilon^{\mu\nu\alpha\beta} u_\alpha M_\beta, \\ H^{\mu\nu} &= D^\mu u^\nu - D^\nu u^\mu + \epsilon^{\mu\nu\alpha\beta} u_\alpha H_\beta, \end{aligned} \quad (9)$$

where

$$P^\mu \equiv -M^{\mu\nu} u_\nu, \quad M^\mu \equiv \frac{1}{2} \epsilon^{\mu\nu\alpha\beta} u_\nu M_{\alpha\beta}, \quad (10)$$

$$D^\mu \equiv H^{\mu\nu} u_\nu, \quad H^\mu \equiv \frac{1}{2} \epsilon^{\mu\nu\alpha\beta} u_\nu H_{\alpha\beta}. \quad (11)$$

In the local rest frame the spatial components \mathbf{P}, \mathbf{M} are the electric and magnetic polarization vectors, respectively. Similarly, the spatial components \mathbf{D} and \mathbf{H} are the electric displacement field and magnetic field intensity, respectively. Note that the minus sign in the definition of P^μ is coming from the fact that the polarization field in the medium points in the direction opposite to the external electric field. Hereafter, we will use $M^{\mu\nu}$ instead of $H^{\mu\nu}$ to discuss the magnetization effects.

Besides the direction given by the fluid velocity, the magnetic field singles out another special direction in the system, which we associate with the spacelike unit vector²

$$b^\mu \equiv \frac{B^\mu}{B}, \quad (12)$$

where

$$B \equiv \sqrt{-B^\mu B_\mu}, \quad b^\mu b_\mu = -1. \quad (13)$$

In a linear approximation we can rewrite M^μ as

$$M^\mu \equiv M b^\mu = \chi_m B^\mu, \quad (14)$$

where

$$M \equiv \chi_m B = \sqrt{-M^\mu M_\mu}. \quad (15)$$

Since $B^\mu B_\mu$ and $M^\mu M_\mu$ are Lorentz scalars, B and M represent the magnitude of the magnetic field and the magnetization in the local rest frame of the fluid, respectively. In addition, χ_m is the magnetic susceptibility, which in principle is a function of temperature and of the magnetic field strength³. As mentioned in the Introduction, we will first consider the case in which χ_m is a constant and subsequently the case in which χ_m has a dependence on temperature.

Although event-by-event simulations of heavy-ion collisions show that the electric field in the laboratory frame could be as large as the magnetic field, we restrict our attention here to the ideal transverse MHD limit. In such a limit, the electric conductivity is assumed to be infinite $\kappa \rightarrow \infty$ (i.e., the medium is a perfectly conducting plasma), thus requiring the electric field to vanish in the comoving frame although the charge current $j^\mu = \kappa E^\mu$ can be finite. Alternatively, this can be seen as a condition on the electric and magnetic fields in the lab frame, \mathbf{E}, \mathbf{B} , which are related via the simple algebraic relation $\mathbf{E} + \mathbf{v} \times \mathbf{B} = 0$, with \mathbf{v} being the three-velocity of the fluid, also in the lab frame. As a result, in the ideal-MHD limit and a linear approximation, the electric polarization vector P^μ and the electric displacement field D^μ can be neglected in Eq. (1).

Under these assumptions, Maxwell's equations simplify considerably, and the first couple of Maxwell equations is given by

$$\epsilon^{\nu\mu\alpha\beta} \partial_\nu F_{\alpha\beta} = 0, \quad (16)$$

or, equivalently

$$\partial_\nu (B^\mu u^\nu - B^\nu u^\mu) = 0. \quad (17)$$

Alternative expressions can be obtained after contracting Eq. (17) with B_μ to obtain

$$\frac{1}{2} (u^\alpha \partial_\alpha) B^2 + B^2 \partial_\alpha u^\alpha + B^2 b^\mu b^\nu \partial_\nu u_\mu = 0, \quad (18)$$

² For completeness, and to avoid confusion, we note that in general relativistic MHD a different notation is normally adopted [see, e.g., Refs. [61, 62]]. First, the signature is spacelike, i.e., $g_{\mu\nu} = (-, +, +, +)$. Second, b^μ is defined as the magnetic field four-vector measured in a comoving frame, while \mathbf{B} still represents the magnetic field three-vector measured by an Eulerian observer. Third, when $M = 0$, the energy-momentum tensor takes the form $T^{\mu\nu} = (e + p + b^2) u^\mu u^\nu + (p + b^2/2) g^{\mu\nu} - b^\mu b^\nu$ [cf. Eq. (30)].

³ From the definition (14) and Eq. (23), χ_m can be obtained through the expansion of the pressure or of the grand canonical potential in the weak-field case, $p(T, B) = p(T, 0) + \chi_m B^2/2 + \mathcal{O}(B^4)$. Unfortunately, χ_m is divergent and is related to the electric charge renormalization in QED [39, 49, 50]. As a result, it is common to define a renormalized magnetic susceptibility, $\tilde{\chi}_m(T) \equiv \chi(T) - \chi(0)$ [50]. In this work, we only consider χ_m as a free parameter, avoiding the difficulties of possible singularities.

or when considering Eq. (17) in the local rest frame, in which case it reduces to the following well-known Maxwell equations

$$\begin{aligned}\nabla \cdot \mathbf{B} &= 0, \\ \partial_t \mathbf{B} &= -\nabla \times \mathbf{E} = \nabla \times (\mathbf{v} \times \mathbf{B}).\end{aligned}\quad (19)$$

Similarly, the second couple of Maxwell equations is instead given by

$$\partial_\mu H^{\mu\nu} = j^\nu, \quad (20)$$

which can be seen as constraint conditions for the charge density and external fields. Because these equations will not be part of our following discussion, we discuss them only briefly. In non-relativistic plasma physics, the charge density j^0 and its time derivative $\partial_t j^0$ are negligible when compared to the other terms in Eqs. (20), so that the latter reduce to Ampere's Law, i.e., $\nabla \times \mathbf{B} = \mathbf{j}$ and to $\nabla \cdot \mathbf{j} = 0$. In relativistic ideal MHD, on the other hand, the fluid is perfectly conducting and E^μ, D^μ, P^μ vanish in the co-moving frame of the fluid, so that Eq. (20) becomes

$$\epsilon^{\mu\nu\alpha\beta} \partial_\mu [u_\beta (B_\alpha - M_\alpha)] = j^\nu. \quad (21)$$

Let us now turn to the thermodynamical relations that will be useful in the remainder of this work. We recall that for a perfect fluid in thermodynamical equilibrium [see, e.g., Refs. [31, 49, 57, 59, 63]]

$$e + p = Ts + \mu n, \quad (22)$$

where n is the baryon number density and μ the associated chemical potential. Furthermore, from the definition of the grand canonical potential $\Omega(T, \mu, B) \equiv -pV$, the magnitude of the magnetic polarization vector is given by

$$M = -\frac{1}{V} \left. \frac{\partial \Omega}{\partial B} \right|_{T, \mu} = \left. \frac{\partial p}{\partial B} \right|_{T, \mu}. \quad (23)$$

This implies that

$$dp = sdT + nd\mu + MdB, \quad (24)$$

and thus that

$$de = Tds + \mu dn - MdB. \quad (25)$$

In ultrarelativistic heavy-ion collisions, the net baryon number density and the chemical potential are vanishingly small at mid-rapidity, therefore, for the sake of simplicity, we will only consider the case of zero baryon chemical potential throughout this work. Then, the thermodynamic relations (22), (24), and (25) reduce to

$$e + p = Ts, \quad (26)$$

$$dp = sdT + MdB, \quad (27)$$

$$de = Tds - MdB, \quad (28)$$

while the sound speed is defined as

$$c_s^2 \equiv \left. \frac{\partial p}{\partial e} \right|_{s, B}. \quad (29)$$

B. Conservation equations and EOS

Inserting the definition of the Faraday tensor (7) into the expression of the (total) energy-momentum tensor Eq. (1), in ideal MHD the latter can be expressed as [58, 59]

$$\begin{aligned}T^{\mu\nu} &= (e + p - MB + B^2)u^\mu u^\nu - (p - MB + \frac{1}{2}B^2)g^{\mu\nu} \\ &\quad + (MB - B^2)b^\mu b^\nu,\end{aligned}\quad (30)$$

where M, B , and b^μ are defined in Eqs. (12), (14), respectively.

The projection of the energy-momentum equation (5) along the four-velocity velocity u^ν expresses the conservation of energy [31] and is given by

$$\begin{aligned}0 &= u_\nu \partial_\mu T^{\mu\nu} \\ &= u^\alpha \partial_\alpha e + (e + p - MB + B^2) \partial_\alpha u^\alpha + Bu^\alpha \partial_\alpha B \\ &\quad + (MB - B^2) u_\mu b^\nu \partial_\nu b^\mu \\ &= u^\alpha \partial_\alpha e + (e + p) \partial_\alpha u^\alpha + Mu^\alpha \partial_\alpha B,\end{aligned}\quad (31)$$

where we have used that $u_\alpha b^\alpha = 0$ and Maxwell's equations (18). Using the thermodynamical relations (28), it is straightforward to conclude that a flow conserves entropy, i.e.,

$$\partial_\mu (su^\mu) = 0, \quad (32)$$

thus confirming that the thermodynamical relations (28) are consistent with the energy-momentum tensor (30) [57–59].

Proceeding in a similar manner, the projection of the conservation equation (5) in the direction orthogonal to the four-velocity u^μ expresses the conservation of momentum [31] and is given by

$$\begin{aligned}0 &= \Delta_{\nu\alpha} \partial_\mu T^{\mu\nu} \\ &= (e + p - MB + B^2) u^\mu \partial_\mu u_\alpha \\ &\quad - \Delta_{\nu\alpha} \partial^\nu (p - MB + \frac{1}{2}B^2) \\ &\quad + \Delta_{\nu\alpha} \partial_\mu [(MB - B^2) b^\mu b^\nu].\end{aligned}\quad (33)$$

Later on, we will show that a Bjorken flow with nonzero magnetization obeys Eq. (33).

The set of equations presented so far needs to be closed by an EOS and because we are here searching for analytic solutions, we have considered two EOSs that are particularly simple. The first one has been adopted already in paper I and is given by

$$e = \frac{1}{c_s^2} p. \quad (34)$$

where the sound speed is $c_s = 1/\sqrt{3}$ when the fluid is ultrarelativistic [31].

Clearly, the EOS (34) is independent of the degree of magnetization or of the strength of the magnetic field, which are however accounted in the second EOS we consider and that is the one for a conformal fluid in a four-dimensional spacetime and in the presence of a magnetic field [57]

$$e = \frac{1}{c_s^2} p - 2MB = 3p - 2MB. \quad (35)$$

The EOS above can be obtained through a conformal transformation [49, 57], or simply by setting to zero the trace of the energy-momentum tensor, i.e., $T^\mu{}_\mu = 0$, and obviously reduces to the ultrarelativistic-fluid EOS in the case of zero magnetization. In Refs. [49, 64], these two EOSs are named respectively EOSs for the “ B -scheme” and the “ Φ -scheme”, since they correspond to a fixed B or a fixed magnetic flux Φ during a conformal (compression) transformation, respectively.

Before concluding this section, we will introduce a very important theorem in ideal MHD, the frozen-flux theorem. With the help of Eq. (17) and entropy conservation (32), we find

$$\Delta_{\mu\nu} u^\alpha \partial_\alpha \left(\frac{B^\mu}{s} \right) = \frac{1}{s} B^\mu \partial_\mu u_\nu, \quad (36)$$

which is the covariant form of the frozen-flux theorem. In the local rest frame it reduces to

$$\frac{\partial}{\partial t} \left(\frac{\mathbf{B}}{s} \right) = \frac{\mathbf{B}}{s} \cdot \nabla \mathbf{v}. \quad (37)$$

In more physical terms, the condition (37) implies that magnetic fields will evolve with the degrees of freedom of the fluid [31, 35, 61, 62].

C. Generalized Bjorken flow

We next discuss the generalization of the Bjorken flow investigated in paper I to the case with nonzero magnetization. Here too, for the sake of finding an analytic solution, we consider a longitudinally boost-invariant Bjorken flow [35, 37], whose four-velocity is

$$u^\mu = \left(\frac{t}{\tau}, 0, 0, \frac{z}{\tau} \right), \quad (38)$$

where $\tau \equiv \sqrt{t^2 - z^2}$ is the proper time. After adopting Milne coordinates, $x^\mu = (\tau, x, y, \eta)$ with

$$\eta \equiv \frac{1}{2} \ln \left(\frac{t+z}{t-z} \right), \quad (39)$$

being the spacetime rapidity. Using such coordinates, the four-velocity simplifies to $u^\mu = (1, \mathbf{0})$, with the directional derivative and four-divergence given respectively by

$$u^\mu \partial_\mu = \partial_\tau, \quad \partial_\alpha u^\alpha = \frac{1}{\tau}. \quad (40)$$

In relativistic heavy-ion collisions, the magnetic field points normally into the transverse direction, i.e., perpendicular to the z direction if this is taken to the beam axis. Hence, we choose the three-vector \mathbf{B} to be parallel to the y direction and homogeneous in the transverse plane, i.e.,

$$\mathbf{B} = B e_y, \quad (41)$$

In this case, the magnetic field does not change in Milne coordinates and the frozen-flux theorem (36) gives

$$\partial_\tau \left(\frac{B}{s} \right) = 0, \quad (42)$$

which implies that B/s is conserved, or more explicitly, that

$$\frac{B}{B_0} = \frac{s}{s_0}, \quad (43)$$

with B_0 and s_0 being the initial magnetic field and the entropy density, respectively. As already mentioned above, the condition (43) means that the magnetic field is advected and distorted by the fluid motion in the same way as a fluid element [35]; identical considerations apply also for astrophysical plasmas, where the rest-mass density is normally used in place of the entropy density [31, 61, 62]. Inserting the velocity from Eq. (38) into Eq. (32), Eq. (43) becomes

$$\frac{B}{B_0} = \frac{s}{s_0} = \frac{\tau_0}{\tau}. \quad (44)$$

thus introducing a simple scaling with proper time.

Finally, let us consider the momentum conservation Eqs. (33), which will ultimately yield the well-known Bjorken scaling law. In the case in which the susceptibility χ_m is a constant, the last term in Eq. (33) reduces to

$$\Delta_\nu^\alpha \partial_\mu [(MB - B^2) b^\mu b^\nu] = (\chi_m - 1) [\partial_\mu (B^\mu B^\alpha) - u_\nu u^\alpha \partial_\mu (B^\mu B^\nu)], \quad (45)$$

Using now the four-velocity (38) and the magnetic field as given by Eqs. (41), (44), it is straightforward to show that such a term vanishes, reducing Eq. (33) to

$$0 = (e + p - MB + B^2) \partial_\tau u_\mu - \Delta_{\nu\mu} \partial^\nu (p - MB + \frac{1}{2} B^2). \quad (46)$$

When $\mu = \eta$, Eq. (46) reads

$$\partial_\eta \left(p - MB + \frac{1}{2} B^2 \right) = 0, \quad (47)$$

thus showing that all thermodynamic variables depend only on the proper time τ , which is the time-honored Bjorken scaling. On the other hand, when $\mu = x, y$, Eq. (46) becomes

$$\partial_\tau u_i - \frac{1}{e + p - MB + B^2} \partial_i \left(p - MB + \frac{1}{2} B^2 \right) = 0. \quad (48)$$

Not surprisingly, when the pressure and the magnetic fields are uniform, the second term in the equation above vanishes, implying that the motion will be geodesic, i.e., with constant velocity.

III. ENERGY-DENSITY EVOLUTION

A. Ultrarelativistic fluid

Using Eq. (31) and the definition of the susceptibility in Eq. (14), the energy conservation equation (31) reads

$$\partial_\tau e + \frac{e + p}{\tau} + \frac{1}{2} \chi_m \partial_\tau B^2 = 0. \quad (49)$$

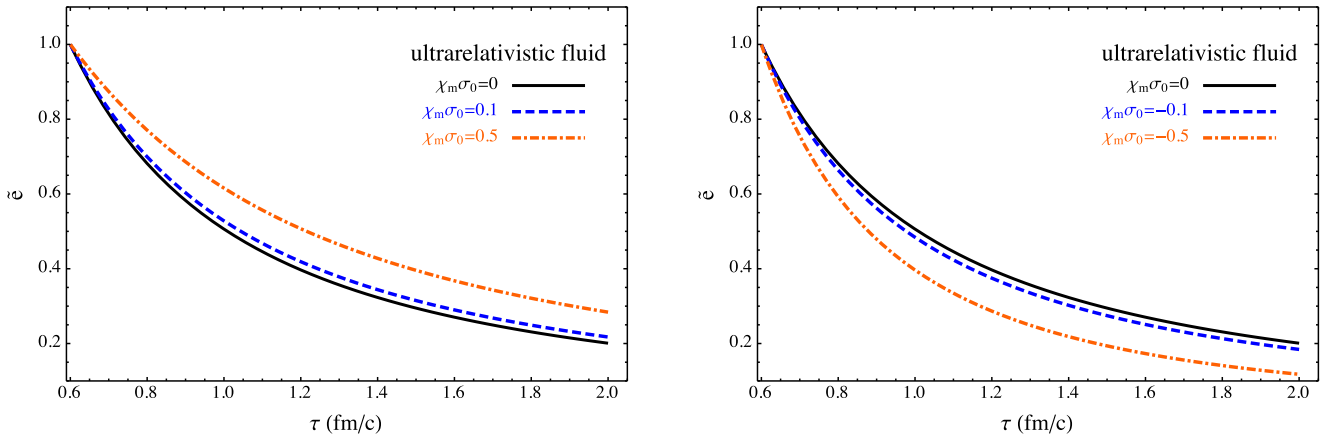


Figure 1: The evolution of the energy density, Eq. (53), with $c_s^2 = 1/3$ and the EOS (34). In the left panel, the solid, dashed, and dash-dotted lines are for $\chi_m \sigma_0 = 0, 0.1, 0.5$, respectively, while in the right panel, the solid, dashed, and dash-dotted lines are for $\chi_m \sigma_0 = 0, -0.1, -0.3$, respectively.

Before we seek for solutions, let us remark that if $\chi_m = 0$ and thus $M = 0$, i.e., if we neglect the magnetization of the fluid, then Eq. (49) is the same as in the standard Bjorken flow without magnetic fields. As discussed in paper I, we would still have the contribution of the magnetic field in the energy-momentum tensor (30), but this would not affect the decay of the energy density [35].

With the help of the frozen-flux theorem (44), Eq. (30) can be rewritten as

$$\partial_\tau e + \frac{e+p}{\tau} - \frac{\chi_m B_0^2}{\tau^3} \tau_0^2 = 0. \quad (50)$$

so that, after introducing the dimensionless quantities

$$\tilde{e} \equiv \frac{e}{e_0}, \quad \sigma_0 \equiv \frac{B_0^2}{e_0}, \quad (51)$$

and using the EOS (34) for an ultrarelativistic fluid, Eq. (50) can be written as

$$\partial_\tau \tilde{e} + (1 + c_s^2) \frac{\tilde{e}}{\tau} - \frac{\chi_m \sigma_0 \tau_0^2}{\tau^3} = 0. \quad (52)$$

Setting as initial condition $\tilde{e}_0 \equiv \tilde{e}(\tau_0) = 1$, the solution of this differential equation is given by

$$\tilde{e}(\tau) = \left(\frac{\tau_0}{\tau}\right)^{1+c_s^2} - \frac{\chi_m \sigma_0}{1-c_s^2} \left[\left(\frac{\tau_0}{\tau}\right)^2 - \left(\frac{\tau_0}{\tau}\right)^{1+c_s^2} \right]. \quad (53)$$

Recalling now that the total energy density is given by the double contraction of the energy-momentum tensor along the four-velocity

$$e_{\text{tot}} \equiv T^{\mu\nu} u_\mu u_\nu = e + \frac{1}{2} B^2 \quad (54)$$

and after introducing the dimensionless total energy density as

$$\tilde{e}_{\text{tot}} \equiv \frac{e_{\text{tot}}}{e_0} = \tilde{e} + \frac{1}{2} \sigma_0 \left(\frac{B}{B_0}\right)^2, \quad (55)$$

the analytic evolution of the energy density in a Bjorken flow with nonzero magnetic susceptibility is given by

$$\tilde{e}_{\text{tot}} = \left(\frac{\tau_0}{\tau}\right)^{1+c_s^2} + \sigma_0 \left\{ \frac{1}{2} \left(\frac{\tau_0}{\tau}\right)^2 - \frac{\chi_m}{1-c_s^2} \left[\left(\frac{\tau_0}{\tau}\right)^2 - \left(\frac{\tau_0}{\tau}\right)^{1+c_s^2} \right] \right\}, \quad (56)$$

showing that, at late times, the energy density decays as $\sim 1/\tau^{1+c_s^2}$.

To better understand the properties of the solution (56) we can take a closer look at the differential equation (49), which tells us that there are two sources to the variation of the energy density. The first one is proportional to $-(e+p)\partial_\alpha u^\alpha = -(e+p)/\tau$ and is related to the expansion of the fluid. It obviously leads to an adiabatic decrease of the energy density. The second term is proportional to $-M\partial_\tau B \propto \chi_m/\tau^3$ and will have a different behaviour depending on the magnetic properties of the fluid. In particular, if the fluid is paramagnetic (i.e., if $\chi_m > 0$), then the fluid will gain energy from the magnetic field and the rate of energy-density decrease will be smaller than without magnetization. On the other hand, if the fluid is diamagnetic (i.e., if $\chi_m < 0$), then the fluid has to spend additional energy to expel the magnetic field, leading to an energy-density decrease that is much faster than without magnetization. This behaviour is summarized in Fig. 1, where we plot the solution (53) for $\chi_m \sigma_0 = 0, \pm 0.1, \pm 0.5$ in the case $c_s^2 = 1/3$. The left panel shows the evolution of the dimensionless energy density relative to a fluid with positive susceptibility ($\chi_m \sigma_0 = 0.1, 0.5$), while the right one refers to a fluid with negative susceptibility ($\chi_m \sigma_0 = -0.1, -0.5$). In both cases, the black lines indicate the case with zero susceptibility, i.e., the classical Bjorken evolution.

B. Magnetized conformal fluid

Next, we turn to discuss the solutions for a fluid with the EOS (35) for a magnetized conformal fluid. In this case, Eqs.

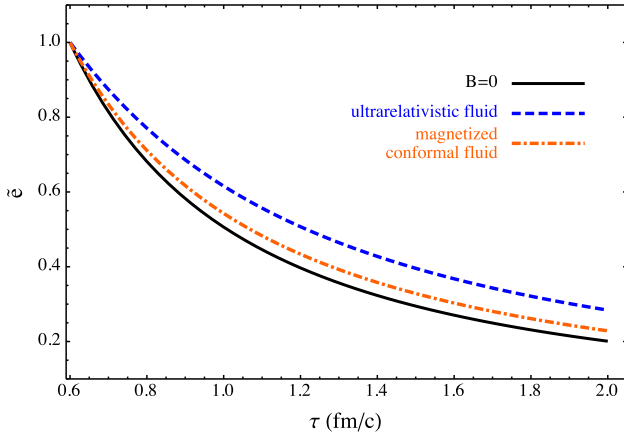


Figure 2: The evolution of the energy density. The black line is the solution without magnetic fields. The dashed and dash-dotted lines are for the solutions for the EOSs considered with $\chi_m \sigma_0 = 0.5$, respectively.

(49) and (50) become

$$\partial_\tau \tilde{e} + \frac{4}{3} \frac{\tilde{e}}{\tau} - \frac{1}{3} \frac{\chi_m \sigma_0}{\tau^3} = 0, \quad (57)$$

whose solution can be found as in the previous case and reads

$$\tilde{e}(\tau) = \left(\frac{\tau_0}{\tau}\right)^{4/3} - \frac{1}{2} \chi_m \sigma_0 \left[\left(\frac{\tau_0}{\tau}\right)^2 - \left(\frac{\tau_0}{\tau}\right)^{4/3} \right], \quad (58)$$

while for the total dimensionless energy density it is given by

$$\tilde{e}_{\text{tot}} = \left(\frac{\tau_0}{\tau}\right)^{4/3} + \frac{\sigma_0}{2} \left\{ \left(\frac{\tau_0}{\tau}\right)^2 - \chi_m \left[\left(\frac{\tau_0}{\tau}\right)^2 - \left(\frac{\tau_0}{\tau}\right)^{4/3} \right] \right\}. \quad (59)$$

Comparing the solution (55) with (58), it is easy to conclude that the solution of a magnetized conformal fluid is the same one as in the case of an ultrarelativistic fluid, which however has smaller effective magnetic susceptibility, i.e., $\chi_m \rightarrow \chi_m/3$. In Fig. 2, we compare the solutions (55) and (58) for the two different EOSs considered. Note that for a positive susceptibility, the fluid with the EOS (35) of a magnetized conformal fluid will gain less energy from the magnetic field than for the EOS (34) of an ultrarelativistic fluid, thus being closer to the case when the magnetic field is absent. One can draw similar conclusions for negative susceptibilities.

IV. ENERGY-DENSITY EVOLUTION WITH AN EXTERNAL MAGNETIC FIELD

A. Ultrarelativistic fluid

We now extend our discussion to case of an external magnetic field which is suitably tuned to decay following a power law in proper time, i.e.,

$$B(\tau) = B_0 \left(\frac{\tau_0}{\tau}\right)^a, \quad (60)$$

where a is a constant and the case $a = 1$ falls back to the case discussed in the previous section [cf. Eq. (44)]. Given the typical and very short timescales involved in heavy-ion collisions, this scenario is rather unrealistic, but we consider it here partly because it has been investigated also in paper I and partly because it allows us to obtain another interesting analytic solution. Another important simplifying assumption is that we will take the external field to be much stronger than any magnetic field produced at the collision. This implies that we can neglect the latter and, more importantly, that such external field does not have to satisfy Maxwell's equations (17) coupled to the fluid.

Under these somewhat academic assumptions, the energy-momentum conservation Eq. (61) with the Bjorken velocity becomes

$$\partial_\tau e + \frac{e + p - MB + B^2}{\tau} + \frac{1}{2} \partial_\tau B^2 = 0. \quad (61)$$

where we used the fact that b^μ is non-vanishing only in the y direction, so that $-B^2 u_\mu b^\nu \partial_\nu b^\mu = 0 = MB u_\mu b^\nu \partial_\nu b^\mu$. Inserting Eq. (60) into Eq. (61) yields

$$\partial_\tau e + \frac{e + p}{\tau} + (1 - a - \chi_m) \frac{B_0^2 \tau_0^{2a}}{\tau^{2a+1}} = 0. \quad (62)$$

It is simple to check that when $a = 1$, Eq. (62) reduces to Eq. (52) and when $\chi_m = 0$, Eq. (62) is also consistent with the results of Ref. [35].

Using the EOS (34), we find

$$\partial_\tau \tilde{e} + (1 + c_s^2) \frac{\tilde{e}}{\tau} + (1 - a - \chi_m) \sigma_0 \frac{\tau_0^{2a}}{\tau^{2a+1}} = 0. \quad (63)$$

The solution is

$$\tilde{e}(\tau) = \left(\frac{\tau_0}{\tau}\right)^{1+c_s^2} - \sigma_0 \frac{1 - a - \chi_m}{1 + c_s^2 - 2a} \left[\left(\frac{\tau_0}{\tau}\right)^{2a} - \left(\frac{\tau_0}{\tau}\right)^{1+c_s^2} \right] \quad (64)$$

for $a \neq (1 + c_s^2)/2$, and

$$\tilde{e}(\tau) = \left(\frac{\tau_0}{\tau}\right)^{1+c_s^2} + \frac{1}{2} \sigma_0 (1 - c_s^2 - 2\chi_m) \left(\frac{\tau_0}{\tau}\right)^{1+c_s^2} \log \left(\frac{\tau_0}{\tau}\right) \quad (65)$$

for $a = (1 + c_s^2)/2$. One can also get Eq. (65) by taking the limit $a \rightarrow (1 + c_s^2)/2$ for the solution (64). The normalized total energy density is then

$$\tilde{e}_{\text{tot}} = \left(\frac{\tau_0}{\tau}\right)^{1+c_s^2} - \sigma_0 \frac{1 - a - \chi_m}{1 + c_s^2 - 2a} \left[\left(\frac{\tau_0}{\tau}\right)^{2a} - \left(\frac{\tau_0}{\tau}\right)^{1+c_s^2} \right] + \frac{1}{2} \sigma_0 \left(\frac{\tau_0}{\tau}\right)^{2a}, \quad (66)$$

for $a \neq (1 + c_s^2)/2$, and

$$\tilde{e}_{\text{tot}} = \left(\frac{\tau_0}{\tau}\right)^{1+c_s^2} + \frac{1}{2} \sigma_0 (1 - c_s^2 - 2\chi_m) \left(\frac{\tau_0}{\tau}\right)^{1+c_s^2} \log \left(\frac{\tau_0}{\tau}\right) + \frac{1}{2} \sigma_0 \left(\frac{\tau_0}{\tau}\right)^{2a}, \quad (67)$$

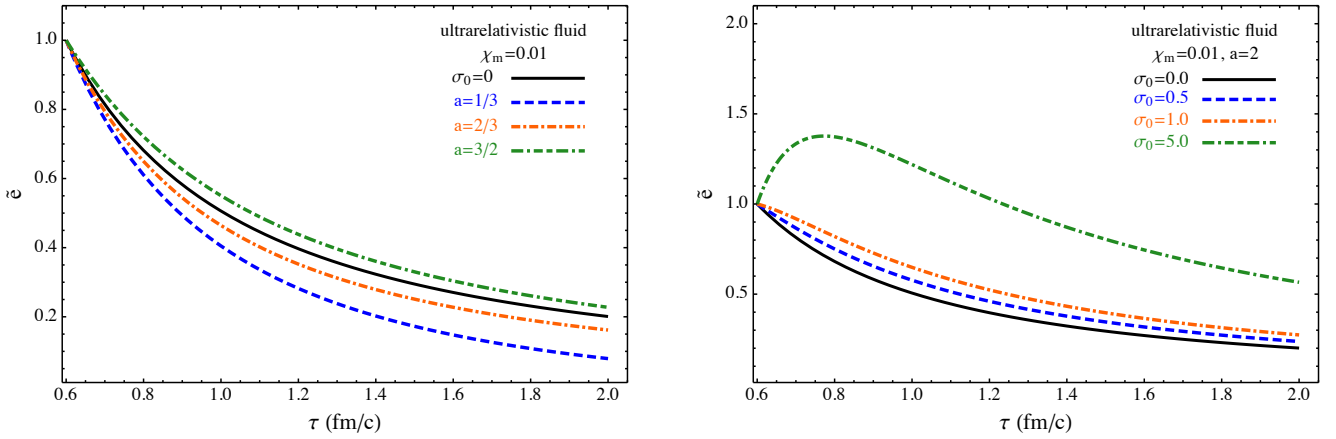


Figure 3: Left panel: the solutions (64), (65) for different values of the parameters. We choose $\chi_m = 0.01$. The black solid line is for the case without magnetic field. For $\sigma_0 = 0.5$, the blue dashed, orange dash-dotted, and green dash-dotted lines are for $a = 1/3, 2/3, 3/2$, respectively. Right panel: the same as in the left panel but for $\chi_m = 0.01$ and $a = 2$. The black solid line is for the case without magnetic fields. The blue dashed, orange dash-dotted, and green dash-dotted lines are for $\sigma_0 = 0.5, 1.0, 5.0$, respectively.

for $a = (1 + c_s^2)/2$.

Since the term $\left[(\tau_0/\tau)^{2a} - (\tau_0/\tau)^{1+c_s^2} \right] / (1 + c_s^2 - 2a)$ is always positive, from Eq. (64) we see that the effect of nonzero magnetization enters only through the prefactor $1 - a - \chi_m$. More precisely, when $a > 1 - \chi_m$, \tilde{e} decays more slowly than in the case without magnetic fields, and when $0 < a < 1 - \chi_m$, \tilde{e} decays faster. One can reach the same conclusion by analyzing the sign of the last term in Eq. (62). We can demonstrate our conclusion in two limits and, for simplicity, we assume $\chi_m > 0$. For $a \rightarrow 0$, the magnetic field is constant in proper time and does not evolve with the fluid. Thus, the fluid energy density must decay faster in order to sustain this constant magnetic field. For $a \rightarrow \infty$, the magnetic field decays very rapidly and its energy will be transferred to the fluid due to the energy-conservation law. So, one can expect a peak of the energy density near the initial time, which is associated with a resistive “reheating” of the fluid [35].

We show these solutions in Fig. 3. Since χ_m is very small for the QGP, we choose a typical value $\chi_m = 0.01$ in the left panel of Fig. 3. The black solid line is for the case without magnetic field, $\sigma_0 = 0$, while the blue dashed, orange dash-dotted, and green dash-dotted lines are for $a = 1/3, 2/3, 3/2$, respectively, for the case $\sigma_0 = 0.5$. For $a > 1 - \chi_m$ the energy density decays more slowly and for $a < 1 - \chi_m$, it decays faster than without magnetization, respectively. In the right panel of Fig. 3, fixing $\chi_m = 0.01$ and $a = 2$, the blue dashed, orange dash-dotted, and green dash-dotted lines are for $\sigma_0 = 0.5, 1.0, 5.0$, respectively. If σ_0 is large enough, we can observe the initial “reheating” effect.

B. Magnetized conformal fluid

We conclude this section by considering the evolution under external magnetic field (60) when the fluid obeys the EOS (35) for a magnetized conformal fluid. In this case, Eq. (62)

becomes

$$\partial_\tau \tilde{e} + \frac{4}{3} \frac{\tilde{e}}{\tau} + \sigma_0 \left(1 - a - \frac{1}{3} \chi_m \right) \frac{\tau_0^{2a}}{\tau^{a+1}} = 0. \quad (68)$$

The solution can be obtained similarly as above and reads

$$\tilde{e}(\tau) = \left(\frac{\tau_0}{\tau} \right)^{4/3} - \frac{\sigma_0}{2} \frac{3 - 3a - \chi_m}{2 - 3a} \left[\left(\frac{\tau_0}{\tau} \right)^{2a} - \left(\frac{\tau_0}{\tau} \right)^{4/3} \right] \quad (69)$$

for $a \neq 2/3$, and

$$\tilde{e}(\tau) = \left(\frac{\tau_0}{\tau} \right)^{4/3} + \frac{\sigma_0}{3} (1 - \chi_m) \left(\frac{\tau_0}{\tau} \right)^{4/3} \log \left(\frac{\tau_0}{\tau} \right) \quad (70)$$

for $a = 2/3$. The normalized total energy density is

$$\tilde{e}_{\text{tot}} = \left(\frac{\tau_0}{\tau} \right)^{4/3} + \frac{\sigma_0}{2} \left\{ \left(\frac{\tau_0}{\tau} \right)^2 - \frac{3 - 3a - \chi_m}{2 - 3a} \left[\left(\frac{\tau_0}{\tau} \right)^{2a} - \left(\frac{\tau_0}{\tau} \right)^{4/3} \right] \right\} \quad (71)$$

for $a \neq 2/3$, and

$$\tilde{e}_{\text{tot}} = \left(\frac{\tau_0}{\tau} \right)^{4/3} + \frac{\sigma_0}{3} (1 - \chi_m) \left(\frac{\tau_0}{\tau} \right)^{4/3} \log \left(\frac{\tau_0}{\tau} \right) + \frac{\sigma_0}{2} \left(\frac{\tau_0}{\tau} \right)^2 \quad (72)$$

for $a = 2/3$. The behaviour of Eq. (69) can be discussed in a manner similar to the previous case of an ultrarelativistic fluid. When $a > 1 - \chi_m/3$, \tilde{e} will decay more slowly than in the case without magnetic field, and when $0 < a \leq 1 - \chi_m/3$, \tilde{e} will decay faster than in the case without magnetic field.

V. ENERGY-DENSITY EVOLUTION WITH TEMPERATURE-DEPENDENT MAGNETIC SUSCEPTIBILITY

After the rather academic discussion of the previous section, we will now consider a more realistic scenario. For the

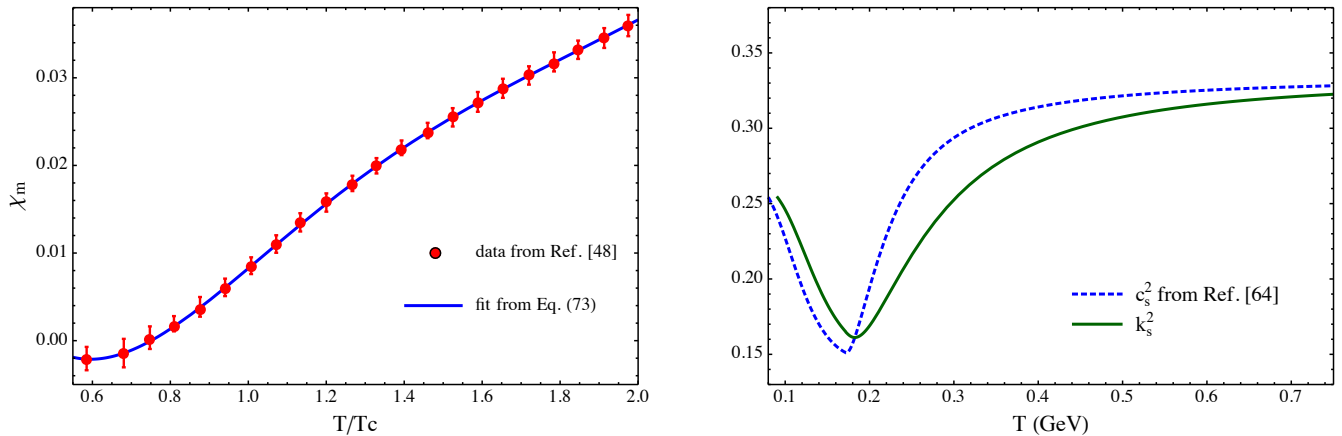


Figure 4: Left panel: magnetic susceptibility χ_m ; the filled red circles refer to the data in Ref. [49], while the solid line shows the fit given by Eq. (73). Right panel: behaviour of $k_s^2 = p/e$ and of c_s^2 . The dashed line shows the speed of sound given by Eq. (77) from the parametrization of Ref. [65]. Finally, the solid green line provides the ratio between the pressure and energy density; note the close similarity between k_s^2 and c_s^2 .

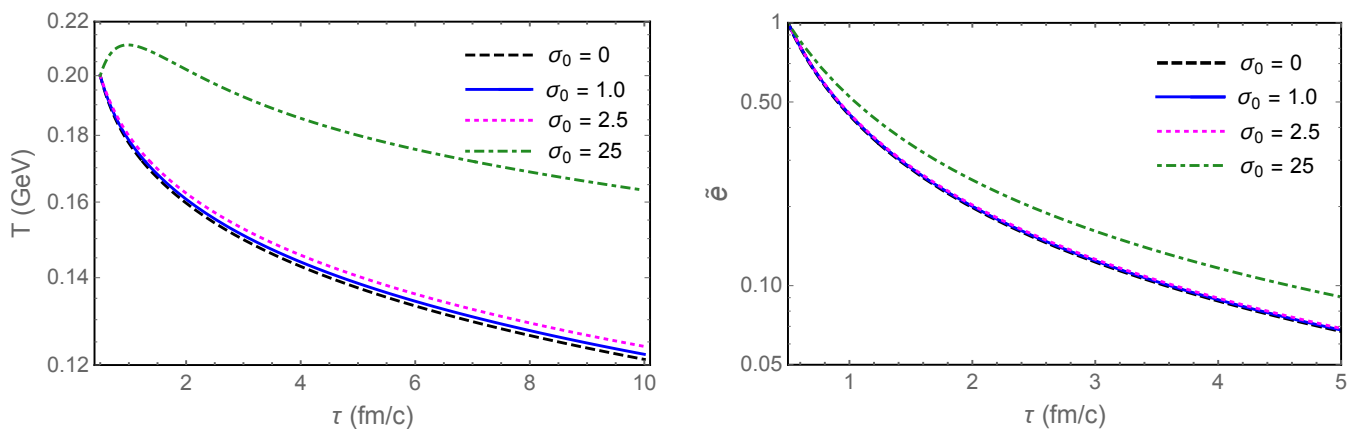


Figure 5: Evolution of temperature T (left panel) and normalized energy density $\tilde{e} = e/e_0$ (right panel) as a functions of proper time τ . We choose initial temperature $T_0 = 200$ MeV, initial time $\tau_0 = 0.5$ fm/c, and critical temperature $T_c = 180$ MeV. The black dashed, blue solid, magenta dotted, and green dot-dashed lines are for $\sigma_0 = 0, 1.0, 2.5, 25$, respectively.

sake of simplicity, we will choose the temperature T as independent variable and express all quantities as a function of T . We also choose the EOS named “*s95n-v1*” parametrization of Ref. [65], which is also obtained from lattice QCD [66]. We will use lattice-QCD data for the magnetic susceptibility χ_m as a function of T and investigate the effect of the magnetization across the deconfinement phase transition.

The behaviour of the magnetic susceptibility as a function of the temperature has been studied in lattice-QCD calculations following several different approaches [see, e.g., Refs. [46, 47, 49, 50]]. Since we concentrate on the deconfinement phase transition and we expect that $\chi_m(T)$ becomes negative in the hadronic phase, we choose the data from Ref. [49]. Noting that a power-law behaviour $(T/T_c - 1)^n$ with $n = \text{const.}$ is typical for quantities near a phase transition, we capture the analytical behaviour of the data by expressing $\chi_m(T)$ as a

polynomial in powers of $T/T_c - 1$, i.e.,

$$\chi_m(T) = \sum_{n=0} c_n \left(\frac{T}{T_c} - 1 \right)^n, \quad (73)$$

where T_c is the transition temperature and the first six coefficients appearing in Eq. (73) are given by $c_0 = 0.0082$, $c_1 = 0.0374$, $c_2 = 0.0039$, $c_3 = -0.0427$, $c_4 = 0.0430$, and $c_5 = -0.0138$.

Similarly, we introduce the parameter k_s^2 , defined as

$$k_s^2(T) \equiv \frac{p}{e}, \quad (74)$$

which is a function of T . Note that k_s^2 is reminiscent of, but distinct from, the square of the sound speed c_s^2 . The latter is in fact defined as in Eq. (29) and will in general be different from the simple ratio of the pressure and energy density [the only exception being the EOS of an ultrarelativistic fluid (34) or the EOS normally used in cosmology $p = we$ [31]]. Hence,

the parameter k_s^2 does not have a precise physical significance, but should be seen mostly as a mathematically convenient definition that allows us to express the pressure in terms of the energy density and hence obtain an analytic solution. Having said that, it is interesting also to remark that k_s^2 and c_s^2 are rather similar, as shown in the right panel of Fig. 4, where we compare our fitting functions for χ_m and k_s^2 with the original data from Refs. [49] and [65].

From the “*s95n-v1*” parametrization of Ref. [65], $p(T)$ and $e(T)$ can be obtained by integrating over the temperature the trace anomaly $\theta(T) \equiv e(T) - 3p(T)$

$$p(T) = T^4 \int_{T_1}^T \frac{\theta(T')}{T'^5} dT', \quad (75)$$

where we choose $T_1 = 1\text{MeV}$ and the trace anomaly is given in Ref. [65]

$$\theta(T) = T^4 \begin{cases} d_2/T^2 + d_4/T^4 + c_1/T^{n_1} + c_2/T^{n_2}, & T \geq T_0, \\ a_1 T + a_2 T^3 + a_3 T^4 + a_4 T^{10}, & T < T_0, \end{cases} \quad (76)$$

with $d_2 = 0.2654\text{ GeV}^2$, $d_4 = 6.563 \times 10^{-3}\text{ GeV}^4$, $c_1 = -4.370 \times 10^{-5}\text{ GeV}^{n_1}$, $c_2 = 5.774 \times 10^{-6}\text{ GeV}^{n_2}$, $n_1 = 8$, $n_2 = 9$, $T_0 = 171.8\text{ MeV}$, $a_1 = 4.654\text{ GeV}^{-1}$, $a_2 = -879\text{ GeV}^{-3}$, $a_3 = 8081\text{ GeV}^{-4}$, $a_4 = -7039000\text{ GeV}^{-10}$. The *ansatz* in Eq. (76) parametrizes lattice-QCD data when $T \geq T_0$, while it parametrizes data for a hadron resonance gas when $T < T_0$. Inserting Eqs. (75), (76) into Eq. (74), we can get an estimate of $k_s^2(T)$.

As shown in Fig. 4, we also obtain the (squared) speed of sound c_s^2 as a function of T from the “*s95n-v1*” parametrization of Ref. [65],

$$c_s^2 = \frac{s}{T} \frac{dT}{ds}, \quad (77)$$

where entropy density $s \equiv (4p + \theta)/T$ is computed from the trace anomaly and Eq. (75).

Since it is not trivial to obtain the energy density e and the entropy density s as functions of T , we will use the thermodynamical relation (28)

$$e = \frac{T s}{1 + k_s^2} = \frac{s_0 \tau_0}{\tau} \frac{T}{1 + k_s^2}, \quad (78)$$

where in the second equality we used the conservation of entropy. Inserting this into the differential equation (50), yields

$$\partial_\tau \left[\frac{T}{(1 + k_s^2)\tau} \right] + \frac{T}{\tau^2} - \frac{\tau_0}{\tau^3} \frac{T_0}{1 + k_s^2(T_0)} \sigma_0 \chi_m = 0. \quad (79)$$

After solving Eq. (79), we can simply obtain the energy density via

$$\tilde{e} \equiv \frac{e(\tau)}{e_0} = \frac{\tau_0}{\tau} \frac{T(\tau)}{T_0} \frac{1 + k_s^2(T_0)}{1 + k_s^2(T(\tau))}. \quad (80)$$

Choosing the initial temperature T_0 , the initial time τ_0 , and the critical temperature T_c as

$$T_0 = 200\text{ MeV}, \quad T_c = 180\text{ MeV}, \quad \tau_0 = 0.5\text{ fm}/c, \quad (81)$$

we solve Eq. (79) numerically and show the results in Fig. 5 for different $\sigma_0 = 0, 1.0, 2.5, 25$, respectively. Note also that the decay of temperature and energy density is slowed down due to the magnetization effect. This is consistent with Eq. (79), which implies that the magnetic field becomes a source to reheat the system.

As a rough estimate, we can evaluate σ_0 in a typical Bjorken flow for the QGP. For 200 AGeV Au-Au collisions, the magnetic field can reach values of $B \sim 10 m_\pi^2 \sim 0.44\text{ GeV}$, while the energy density of the magnetic field will be $\frac{1}{2} B^2 \sim 5\text{ GeV fm}^{-3}$. The initial energy density of the fluid e_0 will be $\sim 10\text{ GeV fm}^{-3}$. Thus we find $\sigma_0 = B_0^2/e_0 \simeq 0.5$, which is close to the value for the blue solid lines in Fig. 5. Overall, this shows that for a Bjorken flow, the magnetization effect of the QGP can be ignored. On the other hand, for an ultra-large magnetic field, e.g., $\sigma_0 = 25$ which corresponds to $B \gtrsim 50 m_\pi^2$, the temperature will increase, and then decrease, i.e., the system is first reheated by the magnetic field. In that case, which is similar to the one shown in Fig. 3, the QGP can survive longer than otherwise expected.

VI. CONCLUSION

We have studied the evolution of the energy density of the QGP produced, for instance, by the collision of two heavy ions, when this is described as a one-dimensional, longitudinally boost-invariant flow with a transverse magnetic field, i.e., a transverse Bjorken flow within the ideal-MHD limit. This represents a rather straightforward extension of our previous work [35] to the case in which the flow has a nonzero magnetization as described via a magnetic susceptibility χ_m , which we have taken to be either constant or to depend on temperature.

Under these conditions for the Bjorken flow, we were able to obtain analytic solutions relative to two different EOSs, i.e., the EOS (34) for an ultrarelativistic fluid and the EOS (35) for a magnetized conformal fluid. Interestingly, we find that all results for a magnetized conformal fluid can be obtained from the solutions for an ultrarelativistic fluid after a simple scaling of the susceptibility, i.e., by replacing $\chi_m \rightarrow \chi_m/3$. We also find that for a paramagnetic fluid, i.e., with $\chi_m > 0$, the fluid gains energy from the decay of the magnetic field, thus with an energy density decaying more slowly than in the case without magnetic fields. On the other hand, for a diamagnetic fluid, i.e., with $\chi_m < 0$, the fluid loses energy to the magnetic field and the energy density will decay more rapidly than in the absence of a magnetic field.

We have also considered the case where the magnetic field is external and very large, with an evolution that follows a power-law behaviour in proper time with exponent a . The solutions in this case can be distinguished in terms of two scenarios. The magnetic field decays more slowly than in the ideal-MHD case for $a > 1 - \chi_m$, while the decay is more rapid for $a < 1 - \chi_m$.

If the magnetic field or, strictly speaking, $\sigma_0 = B_0^2/e_0$, is large enough, the fluid will absorb energy in excess of the decay caused by the expansion. In that case, one will observe a

peak in the energy density at the early stage. This is a resistive “reheating” of the fluid. The amount of this increase depends on the magnetic-field strength and hence will increase with σ_0 and a . However, at late times, its energy density will decrease with an asymptotic rate that is the same as in the Bjorken flow, i.e., $\propto \tau^{-4/3}$.

Finally, we have also considered a temperature-dependent magnetic susceptibility and a realistic equation of state given by lattice-QCD data. We find that the magnetization effect of the QGP will slow down the decay of temperature and energy density. However, for realistic values of the magnetic susceptibility and initial magnetic field, this effect can be ignored, at least in a one-dimensional Bjorken flow. For an ultra-large magnetic field, on the other hand, the system might be reheated and the QGP may survive longer than expected.

Acknowledgments

S.P. and V.R. are supported by the Alexander von Humboldt Foundation, Germany. Partial support comes also from “New-CompStar”, COST Action MP1304, by the LOEWE-Program in HIC for FAIR, and by the NSFC under grant No. 11205150.

Note added – When this work was being completed, we learned that another group, Ref. [67], has investigated within a 3+1-dimensional ideal-hydrodynamics approach the magnetization effects of an external magnetic field on the anisotropic expansion of the QGP.

-
- [1] A. Bzdak and V. Skokov, *Phys.Lett.* **B710**, 171 (2012), 1111.1949.
 - [2] W.-T. Deng and X.-G. Huang, *Phys.Rev.* **C85**, 044907 (2012), 1201.5108.
 - [3] H. Li, X.-l. Sheng, and Q. Wang, (2016), 1602.02223.
 - [4] M. Gyulassy and L. McLerran, *Nucl. Phys.* **A750**, 30 (2005), nucl-th/0405013.
 - [5] D. E. Kharzeev, L. D. McLerran, and H. J. Warringa, *Nucl.Phys.* **A803**, 227 (2008), 0711.0950.
 - [6] K. Fukushima, D. E. Kharzeev, and H. J. Warringa, *Phys.Rev.* **D78**, 074033 (2008), 0808.3382.
 - [7] D. E. Kharzeev and H.-U. Yee, *Phys.Rev.* **D83**, 085007 (2011), 1012.6026.
 - [8] Y. Burnier, D. E. Kharzeev, J. Liao, and H.-U. Yee, *Phys.Rev.Lett.* **107**, 052303 (2011), 1103.1307.
 - [9] M. Stephanov and Y. Yin, *Phys.Rev.Lett.* **109**, 162001 (2012), 1207.0747.
 - [10] J.-W. Chen, J.-y. Pang, S. Pu, and Q. Wang, *Phys.Rev.* **D89**, 094003 (2014), 1312.2032.
 - [11] J.-Y. Chen, D. T. Son, M. A. Stephanov, H.-U. Yee, and Y. Yin, *Phys.Rev.Lett.* **113**, 182302 (2014), 1404.5963.
 - [12] D. T. Son and N. Yamamoto, *Phys.Rev.Lett.* **109**, 181602 (2012), 1203.2697.
 - [13] D. T. Son and N. Yamamoto, *Phys.Rev.* **D87**, 085016 (2013), 1210.8158.
 - [14] J.-H. Gao, Z.-T. Liang, S. Pu, Q. Wang, and X.-N. Wang, *Phys.Rev.Lett.* **109**, 232301 (2012), 1203.0725.
 - [15] J.-W. Chen, S. Pu, Q. Wang, and X.-N. Wang, *Phys.Rev.Lett.* **110**, 262301 (2013), 1210.8312.
 - [16] A. Bzdak, V. Koch, and J. Liao, *Lect.Notes Phys.* **871**, 503 (2013), 1207.7327.
 - [17] D. E. Kharzeev, *Prog.Part.Nucl.Phys.* **75**, 133 (2014), 1312.3348.
 - [18] D. E. Kharzeev, (2015), 1501.01336.
 - [19] R.-H. Fang, J.-H. Gao, S. Pu, and Q. Wang, Chiral kinetic theory and berry phase from quantum kinetic approaches, in preparation.
 - [20] X.-G. Huang and J. Liao, *Phys.Rev.Lett.* **110**, 232302 (2013), 1303.7192.
 - [21] S. Pu, S.-Y. Wu, and D.-L. Yang, *Phys.Rev.* **D89**, 085024 (2014), 1401.6972.
 - [22] Y. Jiang, X.-G. Huang, and J. Liao, *Phys.Rev.* **D91**, 045001 (2015), 1409.6395.
 - [23] S. Pu, S.-Y. Wu, and D.-L. Yang, *Phys.Rev.* **D91**, 025011 (2015), 1407.3168.
 - [24] P. Romatschke and U. Romatschke, *Phys. Rev. Lett.* **99**, 172301 (2007), 0706.1522.
 - [25] M. Luzum and P. Romatschke, *Phys. Rev.* **C78**, 034915 (2008), 0804.4015.
 - [26] H. Song and U. W. Heinz, *Phys.Lett.* **B658**, 279 (2008), 0709.0742.
 - [27] H. Song and U. W. Heinz, *Phys. Rev.* **C78**, 024902 (2008), 0805.1756.
 - [28] B. Schenke, S. Jeon, and C. Gale, *Phys. Rev.* **C85**, 024901 (2012), 1109.6289.
 - [29] V. Roy, A. K. Chaudhuri, and B. Mohanty, *Phys. Rev.* **C86**, 014902 (2012), 1204.2347.
 - [30] H. Niemi, G. S. Denicol, P. Huovinen, E. Molnar, and D. H. Rischke, *Phys. Rev.* **C86**, 014909 (2012), 1203.2452.
 - [31] L. Rezzolla and O. Zanotti, *Relativistic Hydrodynamics* (Oxford University Press, 2013).
 - [32] U. Gursoy, D. Kharzeev, and K. Rajagopal, *Phys. Rev.* **C89**, 054905 (2014), 1401.3805.
 - [33] B. G. Zakharov, *Phys. Lett.* **B737**, 262 (2014), 1404.5047.
 - [34] K. Tuchin, *Phys.Rev.* **C88**, 024911 (2013), 1305.5806.
 - [35] V. Roy, S. Pu, L. Rezzolla, and D. Rischke, (2015), 1506.06620.
 - [36] V. Roy and S. Pu, (2015), 1508.03761.
 - [37] J. D. Bjorken, *Phys. Rev.* **D27**, 140 (1983).
 - [38] L. Landau and E. M. Lifshitz, *Fluid dynamics* (Pergamon, New York, 1959).
 - [39] G. S. Bali, F. Bruckmann, G. Endrodi, and A. Schafer, *Phys. Rev. Lett.* **112**, 042301 (2014), 1311.2559.
 - [40] B. L. Ioffe and A. V. Smilga, *Nucl. Phys.* **B232**, 109 (1984).
 - [41] G. S. Bali *et al.*, *Phys. Rev.* **D86**, 094512 (2012), 1209.6015.
 - [42] P. V. Buividovich, M. N. Chernodub, E. V. Luschevskaya, and M. I. Polikarpov, *Nucl. Phys.* **B826**, 313 (2010), 0906.0488.
 - [43] M. Frasca and M. Ruggieri, *Phys. Rev.* **D83**, 094024 (2011), 1103.1194.
 - [44] C. Bonati, M. D’Elia, M. Mariti, F. Negro, and F. Sanfilippo, *Phys.Rev.Lett.* **111**, 182001 (2013), 1307.8063.
 - [45] C. Bonati, M. D’Elia, M. Mariti, F. Negro, and F. Sanfilippo, *PoS LATTICE2013*, 184 (2014), 1312.5070.
 - [46] L. Levkova and C. DeTar, *Phys. Rev. Lett.* **112**, 012002 (2014), 1309.1142.
 - [47] C. Bonati, M. D’Elia, M. Mariti, F. Negro, and F. Sanfilippo, *Phys. Rev.* **D89**, 054506 (2014), 1310.8656.

- [48] Yu. A. Simonov and V. D. Orlovsky, *JETP Lett.* **101**, 423 (2015), 1405.2697.
- [49] G. S. Bali, F. Bruckmann, G. Endrodi, S. D. Katz, and A. Schafer, *JHEP* **08**, 177 (2014), 1406.0269.
- [50] K. Kamikado and T. Kanazawa, *JHEP* **01(2015)129**, 01129 (2014), 1410.6253.
- [51] O. Bergman, G. Lifschytz, and M. Lippert, *JHEP* **05**, 007 (2008), 0802.3720.
- [52] A. Cherman, T. D. Cohen, and E. S. Werbos, *Phys. Rev.* **C79**, 045203 (2009), 0804.1096.
- [53] T. Steinert and W. Cassing, *Phys. Rev.* **C89**, 035203 (2014), 1312.3189.
- [54] D. N. Kabat, K.-M. Lee, and E. J. Weinberg, *Phys. Rev.* **D66**, 014004 (2002), hep-ph/0204120.
- [55] M. M. Anber and M. Unsal, *JHEP* **12**, 107 (2014), 1309.4394.
- [56] A. N. Tawfik and N. Magdy, *Phys. Rev.* **C90**, 015204 (2014), 1406.7488.
- [57] M. M. Caldarelli, O. J. C. Dias, and D. Klemm, *JHEP* **03**, 025 (2009), 0812.0801.
- [58] M. Gedalin and I. Oiberman, *Phys. Rev. E* **51**, 4901 (1995).
- [59] X.-G. Huang, M. Huang, D. H. Rischke, and A. Sedrakian, *Phys. Rev.* **D81**, 045015 (2010), 0910.3633.
- [60] S. R. de Groot, *The Maxwell equations :non-relativistic and relativistic derivations from electron theory* (North-Holland Pub. Co, 1969).
- [61] B. Giacomazzo and L. Rezzolla, *J. Fluid Mech.* **562**, 223 (2006), gr-qc/0507102.
- [62] B. Giacomazzo and L. Rezzolla, *Class. Quant. Grav.* **24**, S235 (2007), gr-qc/0701109.
- [63] L. Landau, E. Lifshitz, and L. Pitaevskii, *Electrodynamics of continuous media. Course of theoretical physics* (Butterworth-Heinemann, Oxford U.K., 1995).
- [64] G. Bali, F. Bruckmann, G. Endrodi, F. Gruber, and A. Schafer, *JHEP* **1304**, 130 (2013), 1303.1328.
- [65] P. Huovinen and P. Petreczky, *Nucl. Phys.* **A837**, 26 (2010), 0912.2541.
- [66] A. Bazavov *et al.*, *Phys. Rev.* **D80**, 014504 (2009), 0903.4379.
- [67] L.-g. Pang, G. Endrodi, G. di, and H. Petersen, (2016), 1602.06176.